Available online at www.sciencedirect.com
ScienceDirect
Journal of the European Ceramic Society 30 (2010) 1059–1065
www.elsevier.com/locate/jeurceramsoc

Effect of the specimen size on strength of Si_3N_4 + SiC composite

Lucia Hegedűsová *, Monika Kašiarová, Erika Csehová, Ján Dusza

Institute of Materials Research, Slovak Academy of Sciences, Watsonova 47, 040 01 Košice, Slovak Republic

Received 30 March 2009; received in revised form 15 September 2009; accepted 28 September 2009
Available online 12 November 2009

Abstract

Bending and contact strength of a recently developed carbon derived Si_3N_4 + SiC micro/nanocomposite have been investigated in four-point and opposite sphere modes using specimens with two different sizes of 3 mm × 4 mm × 45 mm and 1 mm × 2 mm × 20 mm. The fracture origins during bending test were clusters of pores and large SiC grains with different size, shape and location, which resulted in relatively low strength (675 MPa and 832 MPa) and Weibull moduli (6.4 and 8.6). The fracture origins in specimens tested in contact mode were cone cracks, originated and arised during the loading, and their similar size and shape, together with the preexisting stress field resulted in high strength (1167 MPa and 1997 MPa) and relative high Weibull moduli (17 and 15). In agreement with the theory, bending test specimens with smaller effective volume exhibited higher strength. In contact test, interaction of cone cracks occured in the small specimens at lower load as in larger one, which resulted in the lower strength of small specimens.

Keywords: Si_3N_4; SiC; Composites; Strength; Fracture

1. Introduction

Different approaches have been used during the last decades with the aim to improve the room and high temperature properties, reliability and lifetime of silicon nitride based structural ceramics.[1–3] Using the "nanoparticle strengthening" approach Si_3N_4–SiC nanocomposites have been developed in which nano-sized SiC particles are dispersed in the Si_3N_4 matrix which usually are located either intragranularly, with a size of approximately 30–40 nm, or intergranularly, with a size of approximately 150–170 nm.[4,5]

The influence of the composition and residual stresses on the mechanical properties of Si_3N_4–SiC nanocomposites have been studied by a number of authors during the last 15 years.[5,6] Cheong et al.[7] found a very high room temperature strength of a Si_3N_4–20 vol.% SiC nanocomposite with Y_2O_3 + Al_2O_3 as sintering additives, however, a strength degradation occurred at temperatures higher as 1000 °C. Nanocomposite with 4 wt.% Y_2O_3 of sintering additive had the lower room temperature strength (approximately 1 GPa). However, this value of strength remained up to 1400 °C due to the direct bond of the intergranularly located SiC particles to the Si_3N_4 matrix and due to the inhibition of grain boundary sliding and cavity formation. Dusza and Šajgalík reported an increase in strength and Weibull modulus from 987 MPa to 1203 MPa and from 6.7 to 19, respectively, by the addition of 10% SiC to silicon nitride in a SiCN-derived nanocomposite.[8] The good strength characteristics were associated with a fine and defect-free microstructure.

Usually the strength of ceramic materials is measured by bending test, resulting in a stress state represented by an uniaxial stress with a relatively small gradients.[9–11]

Considering practical applications, the mechanical loading is often represented by a multi-axial stress state to be significantly non-homogeneous. With regard to the determination of the strength of ceramic materials under such a conditions the multi-axial and non-homogeneous stress state can be obtained using contact loading by line or point loads. During the last decades numerous authors investigated the character of the damage introduced during the Hertzian indentation in glasses and different monolithic and composite ceramics.[12–20] A great advantage of the Hertzian indentation test is that the deformation in the substrate produced by the indenter is wholly elastic until fracture occurs and the complications associated with the residual stresses do not exist. Various forms of cone cracks are observed and analyzed in brittle materials when indenter

* Corresponding author. Tel.: +421 55 79 22 416; fax: +421 55 79 22 408.
E-mail addresses: lucia.hegedusova@yahoo.com, lhegedusova@imr.saske.sk (L. Hegedűsová).

0955-2219/$ – see front matter © 2009 Elsevier Ltd. All rights reserved.
doi:10.1016/j.jeurceramsoc.2009.09.026

in the form of conical, spherical, or cylindrical are used called as "the Hertzian cone crack." Lawn has investigated cone cracks developing from the free surface in spherical indentation[13,14] and method for determination of the fracture toughness of brittle material based on the length of the induced cone cracks from a spherical indentation tests was suggested in Refs.[15,17]. Hertzian indentation technique was used to measure surface flaw sizes on polished ceramics and fracture toughness of different ceramics.[19] Finite element method has been used by Kocer and Collins[20] to model the growth of cracks in the Hertzian stress fields and was found that the angle of the cone crack, as grown in the model, is in excellent agreement with observations on experimentally grown cone cracks in glass, with the same Poisson's ration.

The multi-axial and non-homogeneous stress state was induced by line or point contact loading obtained by two opposite rollers or spheres by Fett et al. during the last decade.[21–23] Application of symmetric sphere loading leads to even better defined mechanical boundary conditions compared to the flat supported specimen loaded by one sphere only. Fett et al. calculated the stress solution for loading between opposite rollers and successfully applied the rollers on rollers and spheres on spheres contact strength techniques for the characterization of strength and fatigue of brittle materials.[24–27]

Direct comparison of opposite spheres contact strength test and bending test is difficult however the clarification of the character and mechanisms of fracture origins and their influence on mean strength and the scatter of the strength in new structural ceramics seem to be important.

The aim of the present contribution is to investigate and to compare the strength and fracture behavior of a carbon derived Si_3N_4–SiC micro/nanocomposite using bending and opposite spheres contact strength methods and specimens with different sizes/effective volumes.

2. Experimental procedure

The studied C-derived Si_3N_4–SiC micro/nanocomposite, with the composition listed in Table 1, was prepared at the Institute of Inorganic Chemistry, Slovak Academy of Sciences in Bratislava. The sample contained SiO_2 and C with the aim to achieve 5 wt.% of SiC by carbothermal reduction of SiO_2 after densification. The starting mixtures were homogenized in polyethylene bottle with Si_3N_4 spheres in isopropanol for 24 h. The dried mixture was sieved through 25 μm sieve in order to eliminate large hard agglomerates. Green discs with a diameter of 48 mm and 5 mm thick were die pressed under the pressure of 30 MPa. Green discs were then embedded into a BN powder bed and positioned into a graphite uniaxial die. Samples were hot-pressed under a specific atmosphere, mechanical pressure, and heating regime at 1750 °C for 2 h.

Table 1
Composition of the starting mixture.

	Compound			
	Si_3N_4	Y_2O_3	C	SiO_2
Content (wt.%)	84.1	4.4	4.1	7.4

The microstructure of the nanocomposite was characterized by X-ray diffractometry (XRD), scanning electron microscopy (SEM), and TEM/HREM. XRD analysis was carried out using a Philips X-part diffractometer equipped with a CuK_2 radiation source. Polished and plasma-etched sections of the bulk materials were examined in SEM. To prevent surface charging during examination, the samples were coated with a thin layer of gold. The overall structural and chemical characterization of each specimen was carried out by conventional and analytical TEM investigation with a JEOL 2010 microscope equipped with an ultra-thin window for energy-dispersive X-ray spectrometer.

Thirty specimens with the size of 3 mm × 4 mm × 45 mm and 1 mm × 2 mm × 20 mm were tested in four-point bend on fixture with spans 20 mm/40 mm and 9 mm/18 mm, respectively. Before testing, the specimens were ground to a 15 μm by a diamond grinding wheel. Both edges on the tensile surface were rounded with a radius of about 0.15 mm in order to eliminate failure from the edges of the specimens. The specimens were broken at a cross-head speed of 0.5 mm/min in ambient air.

The characteristic strength $\sigma_{0,bend}$ was determined by four-point bending test and statistically analyzed by Weibull analysis

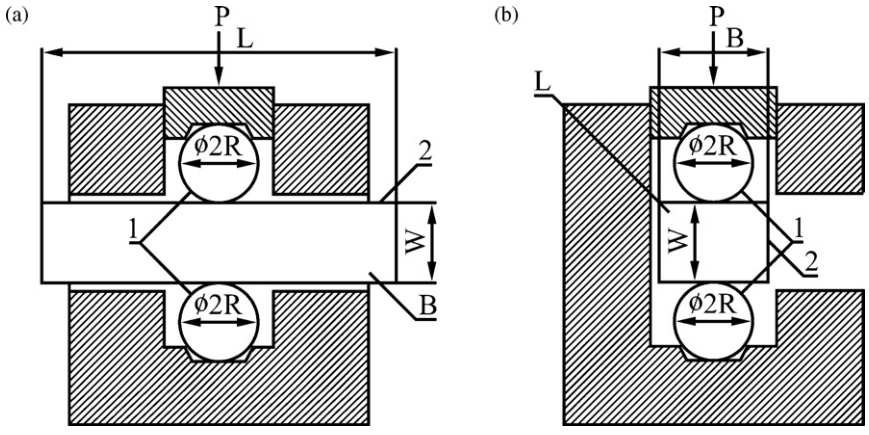

Fig. 1. Characteristic microstructure of the Si_3N_4 + SiC micro/nanocomposite (a) low magnification and (b) high magnification, plasma-etched, SEM.

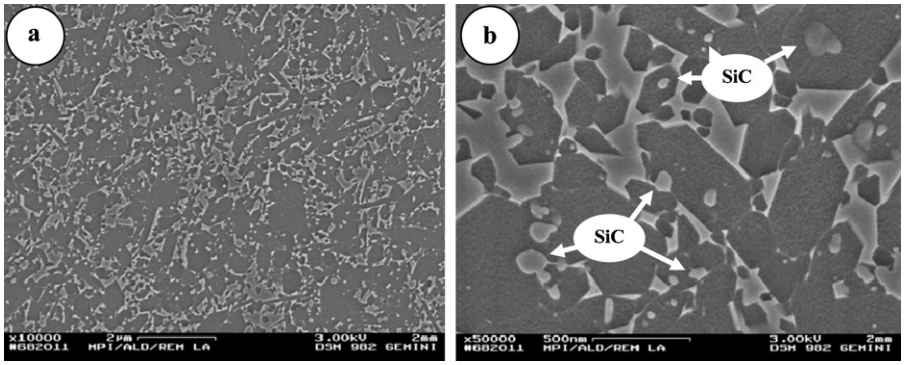

Fig. 2. Schematical illustration of the testing fixture for contact strength test "shperes on spheres".

considering the measured stress σ_{bend} in the form

$$\sigma_{0,cont} = \frac{3P(S_1 - S_2)}{2BW^2}, \quad (1)$$

where B and W are width and height of a specimen, respectively.

The opposite sphere contact strength test (Fig. 1) was realized, using the part of specimens after the bending strength test at the loading rate of 0.5 mm/min. The strength was calculated according to the Eq. (2).

$$\sigma_{max} = \frac{1 - 2\nu_2}{3\pi}\left(\frac{6PE'^2}{R^2}\right)^{1/3}, \quad \frac{1}{E'} = \frac{1 - \nu_1^2}{E_1} + \frac{1 - \nu_2^2}{E_2}, \quad (2)$$

where E_1, ν_1, are the elastic constants of the spheres and E_2, ν_2 the related parameters of the ceramic materials.[23]

The characteristic strength and Weibull modulus were computed using two-parameter Weibull theory and maximum likelihood method.[11]

After the bending and contact strength tests fractographic methods have been used with the aim to identify and to describe the fracture origins and the fracture process during the tests.[28,29]

3. Results and discussion

3.1. Microstructure

The characteristic microstructure of the experimental material is illustrated in Fig. 2a and b. The microstructure analysis using ceramography and SEM revealed that technological defects are present in the form of clusters of SiC and porosity in the material only randomly. The Si_3N_4–SiC nanocomposite consists of a very fine, homogeneously distributed Si_3N_4 grains with a low aspect ratio. Globular nano- and submicron-sized SiC particles are located intragranularly in the Si_3N_4 grains or intergranularly between the Si_3N_4 grains. It was difficult to distinguish between the SiC particles located integranularly and the grain boundary phase because they are similarly affected by plasma etching. The mean diameter of Si_3N_4 grain is 140 nm and grains with a diameter larger than 500 nm were observed in the microstructure only occasionally. The volume fraction of the SiC nanoparticles can be estimated approximately as 5 vol.%. X-ray analysis revealed that the main phase in material is β-Si_3N_4 with a small amount of β-SiC. Beside the Si_3N_4 and SiC, some additional crystalline phases were detected in the composite, mainly Y_2SiO_7 and Si_2N_2O.

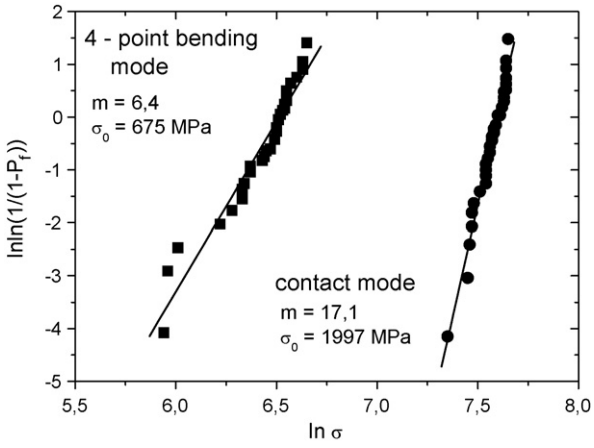

Fig. 3. Weibull distribution of the strength values of standard specimens tested in bending and in contact mode.

3.2. Weibull parameters and fracture origins

Weibull distribution of the measured four-point flexure strength values of the investigated nanocomposite with the specimen effective volume of 18.4 mm^3 is illustrated in Table 2 and

Table 2
Weibull parameters of the composite in bending and contact mode for specimens with different sizes.

Method/Weibull parameters	Bending/standard 3 × 4 × 45 (mm)	Bending/small 1 × 2 × 20 (mm)	Contact/standard 3 × 4 × 45 (mm)	Contact/small 1 × 2 × 20 (mm)
Characteristic strength (MPa)	675	832	1997	1167
Weibull modulus	6.4	8.6	17.1	15.0

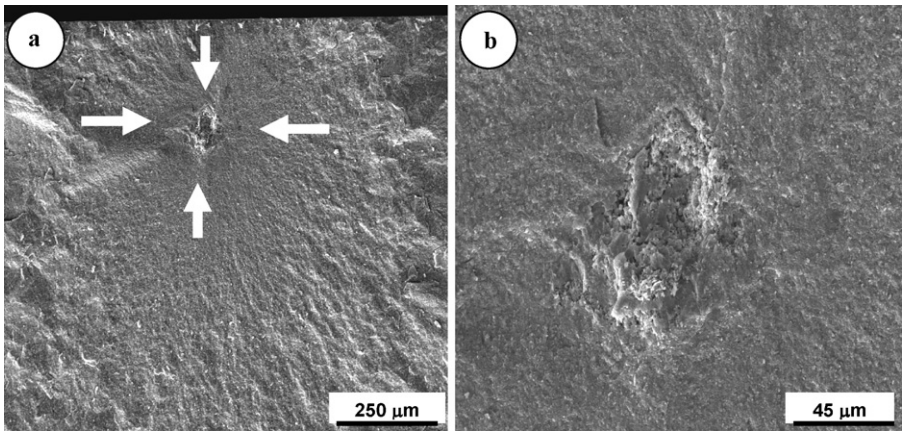

Fig. 4. Characteristic fracture origin in standard specimens tested in bending.

Fig. 3a. Using the two-parameter Weibull statistics the characteristic strength of material was $\sigma_0 = 675$ MPa and Weibull modulus was $m = 6.4$. Slightly higher value of characteristic strength $\sigma_0 = 832$ MPa and Weibull modulus $m = 8.6$ was obtained tested the specimens with effective volume of 1.55 mm^3.

Weibull distribution of the measured contact strength values of the investigated nanocomposite with the specimen effective volume of 18.4 mm^3 is illustrated in Table 2 and Fig. 3b. Using the two-parameter Weibull statistics the characteristic strength of material was $\sigma_0 = 1997$ MPa and Weibull modulus was $m = 17.1$. Lower value of characteristic strength $\sigma_0 = 1167$ MPa and similar Weibull modulus $m = 15$ was obtained tested the specimens with effective volume of 1.55 mm^3.

The characteristic strength and Weibull modulus of the carbon derived composite are lower in comparison with the parameters of the SiCN-derived Si_3N_4–SiC micro/nanocomposite tested in bending.[30] Fractographic analysis of the fracture surface of failed specimens revealed that the reason of the lower characteristic strength of carbon derived composite compared to the strength of the SiCN-derived materials is the presence of processing flaws in the investigated material. In most cases the location of the fracture origins/flaws were in the volume of the specimens, but they were also located near the surface, on the surface, and at the edges/surface (Fig. 4a and b). Fracture origins were in all cases processing flaws and machining induced flaws were not found. Study of the size and shape of the fracture origins revealed that their size was usually up to 60 μm, with the mean value of half-minor axis length of about 35 μm. Their shape was mostly elliptical, but circular-shaped fracture origins were also observed. In the majority of cases it was easy to define the shape of the defects at least in two-dimension form. Fractographic analysis of the fracture surfaces of failed specimens combined with EDX analysis revealed two main types of processing flaws acting as a failure initiating flaws in the studied material. The first type of fracture origin was a porous region, often connected with another type of flaws. The second type of fracture origins was a cluster of large SiC grains.[31]

The fracture origins after testing the specimens with a dimension of 1 mm × 2 mm × 20 mm were the same volume defects as described above, but they were located mainly at the tensile surface or close to the tensile surface of the specimen (Fig. 5).

According to the result of ceramographic/fractographic examination the fracture during the contact strength test "between spheres" has been initiated under the surface of the specimens and the fracture site is not connected with technological defect. In this case the fracture is caused by creation and growth of the cone cracks during the test up to the critical size (Fig. 6). The higher Weibull moduli (the lower scatter in the strength values) in contact strength test between spheres is caused by the cone cracks of similar size and shape at the failure.

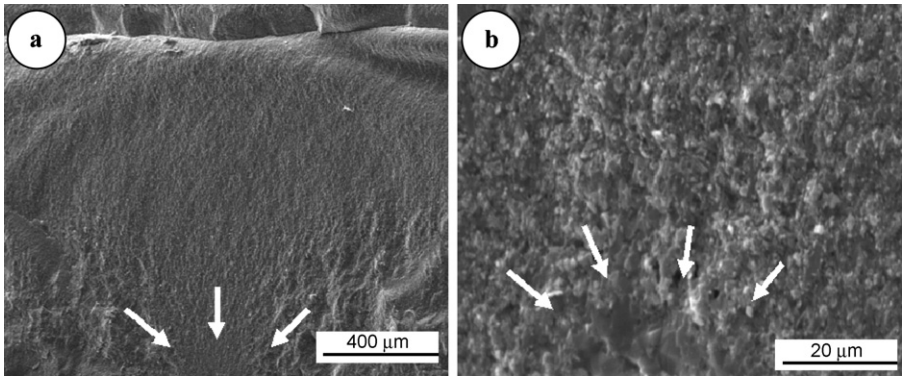

Fig. 5. Characteristic fracture origin in small specimens tested in bending.

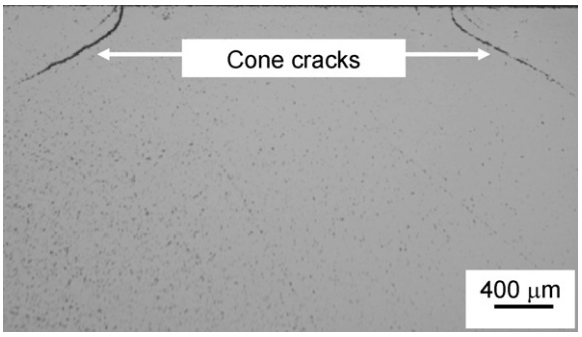

Fig. 6. Cone crack formation during the load in contact strength test.

3.3. Effective volume/surface and bending strength

As it was explained in several publications a very useful concept of Weibull statistics is the effective volume, which permits an easy rapid comparison of the strength of different-sized specimens.[32] For a uniform tension specimen the effective volume is equal to the actual volume in the gage length, $V_{\mathrm{ETensile}} = V$. However the strength test is very often realized in bending mode, similarly as in the present contribution. If a bend specimen has a maximum (outer fiber) stress of σ_{outer} on it, this stress is equivalent (same probability of failure) to a tensile specimen with the same stress, but with an effective volume only, which varies with the Weibull modulus. In the case of a 1/4 four-point rectangular specimen the effective volume is

$$V_{E4B} = \frac{V(m+2)}{4(m+1)^2}, \tag{3}$$

where m is the Weibull modulus and V is the volume of the specimen within the fixture support span.

In the case when the fracture origins are located at the surface of the specimens the Weibull integration should be over the stressed surface and in this case it can be shown that the effective surface for 1/4 four-point specimen is

$$S_{E4B} = \frac{S(m+2)^2}{4(m+1)^2} \tag{4}$$

where S is the surface of the specimen within the fixture support span.

For specimens used in the present investigation this results in the effective volume of the standard specimen $V_{E4B\mathrm{stand}} = 18.4\,\mathrm{mm}^3$ and of small specimen $V_{E4B\mathrm{small}} = 1.55\,\mathrm{mm}^3$ and effective surfaces of the standard specimen $S_{E4B\mathrm{stand}} = 188.13\,\mathrm{mm}^2$ and of small specimen $S_{E4B\mathrm{small}} = 45.72\,\mathrm{mm}^2$, respectively. From these results is evident that the ratio of the effective surface/effective volume for small specimen (approx. 34) is significantly higher compared to this ratio for standard specimen (approx. 10). Probably this is the reason that in the small specimens the surface related defects/fracture origins occured more frequently and the volume defects, located with a certain distance from the tensile surface of the specimens less frequently than in standard specimens. According to the fractographical results the sub-surface located defects were smaller with similar size which probably results in the higher strength and Weibull modulus in comparison to the standard specimens.

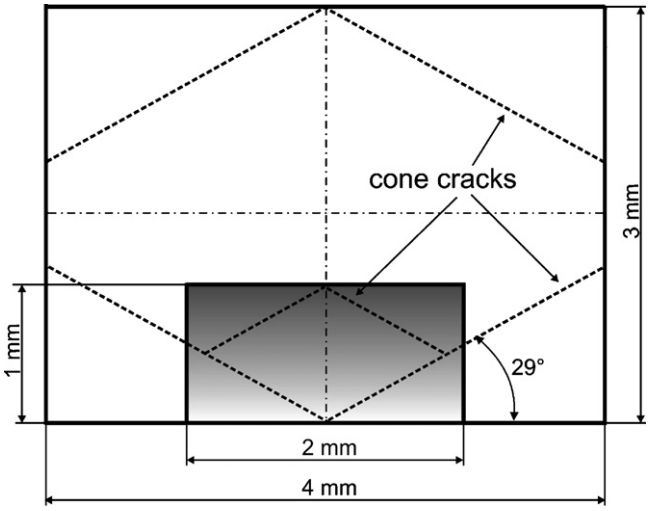

Fig. 7. Schematic illustration of the cone cracks propagation and their mutual interaction or interaction with the side of the specimen in the case of standard and small specimens.

3.4. Specimen size and contact strength

Very high strength and Weibull modulus were obtained during the contact strength test of the material between spheres, $\sigma_{0,\mathrm{stand}} = 1997\,\mathrm{MPa}$ and $m_{\mathrm{stand}} = 17.1$ for the specimens with larger volume and $\sigma_{0,\mathrm{small}} = 1167\,\mathrm{MPa}$ and $m_{\mathrm{small}} = 15$ for the specimens with smaller volume, respectively (Table 2). Fett et al.[29] investigated the strength behavior of different alumina ceramics in bending and contact mode and found significantly higher Weibull exponents m in contact loading test and the characteristic strengths in contact loading was higher by a factor of 4–5 than those for bending. They studied the conditions for the stable and un-stable cone cracks propagation in these materials and found that the cone crack propagation at small cone crack sizes is stable, since the load must increase for increasing cracks. For larger crack lengths, the influence of the interaction of the two cone cracks and interaction of the cone cracks with the free side surfaces of the specimens can cause the catastrophic failure. It seems that there are 3 possibilities for the specimen failure in contact test between spheres. The first and second (for small specimens), when the two cone crack systems mutually interact or interact with the specimen sides. Third, in the case of large specimens when failure of the whole specimen occurs after the strong damage of the contact region. Our experiment illustrated that in opposite sphere contact strength test using specimens of different sizes the failure takes place in different ways. At the beginning in small as well as in larger specimen cone cracks originated with the angle of 29° and extended during the increasing load. In the case of the specimens with size of $W = 3$ mm and $B = 4$ mm and length of 20 mm (see Fig. 7) no mutual cone cracks interaction could occurred and the cracks interacted the specimen side at the crack length of $c = B/2 \cos 29^\circ = 2.29$ mm, if the cone cracks did not reach the critical size before.[33]

In the case of the small specimens with $W = 1$ mm and $B = 2$ mm the cracks probably mutually interact at the crack length of approximately $c_{small} = W/2 \sin 29^\circ = 0.52$ mm.

Probably this is the reason of the lower contact strength of the material tested using the small specimens. The above consideration is valid however in the case of straightforward crack growth only. According to our results, in agreement with the results of the literature, the cone cracks can change their direction during their growth.[28] The reduced scatter in contact strength tests using both specimens dimension can be interpreted as a consequence of the extension of cone cracks, developed during the sphere loading as well as the similar critical crack sizes.

4. Conclusions

Bending and contact strength of a carbon derived in situ reinforced Si_3N_4–SiC micro/nanocomposite have been investigated. The following main results were found:

- The Weibull parameters in bending were $\sigma_0 = 675$ MPa/$\sigma_0 = 832$ MPa and 6.4/8.6 and in contact sphere on sphere test $\sigma_0 = 1997$ MPa/$\sigma_0 = 1167$ MPa and $m = 17.1/m = 15$ for specimens with standard and small specimens size, respectively;
- The Weibull parameters in bending mode were determined by processing related defects—fracture origins, located in bulk and at sub-surface of the specimens. The material tested using specimens of smaller size exhibited higher characteristic strength as well as Weibull modulus due to the smaller and more uniform fracture origin;
- The Weibull parameters in contact mode were determined by cone cracks, originated and arised during the increasing load and results in high Weibull moduli. The interaction of cone cracks in specimen with smaller dimension resulted in lower contact strength.

Acknowledgements

This work was supported by the Slovak Research and Development Agency under the contracts No. APVV-0034-07, No. COST-0042-06, by the Slovak Grant Agency VEGA 2/7194/27, by NANOSMART Centre of Excellence, Slovak Academy of Sciences, by HANCOC-MNT.ERA-NET, and by COST Action 539, by APVV LPP-0203-07. Authors thank T. Fett for his helpful discussion.

References

1. Evans, A. G., Perspective on the development of high-toughness ceramics. *J. Am. Ceram. Soc.*, 1990, **73**, 187–206.
2. Becher, P. F., Sun, E. Y., Plucknett, K. P., Alexander, K. B., Hsueh, Ch. H., Lin, H. T., Waters, S. B. and Westmoreland, C. G., Microstructural design of silicon nitride with improved fracture toughness. I. Effects of grain shape and size. *J. Am. Ceram. Soc.*, 1998, **81**, 2821–2830.
3. Harmer, M. P., Chan, H. M. and Miller, G. A., Unique opportunities for microstructural engineering with duplex and laminar ceramic composites. *J. Am. Ceram. Soc.*, 1992, **75**, 1715–1728.
4. Niihara, K., New design concept of structural ceramics: ceramic nanocomposites: composites. *J. Ceram. Soc. Jpn.*, 1991, **99**, 974–982.
5. Sternitzke, M., Structural ceramic nanocomposites. *J. Eur. Ceram. Soc.*, 1997, **17**, 1061–1082.
6. Herrmann, M., Schubert, C., Rendtel, A. and Hübner, H., Silicon nitride/silicon carbide nanocomposite materials. I. Fabrication and mechanical properties at room temperature. *J. Am. Ceram. Soc.*, 1998, **81**, 1095–1108.
7. Cheong, D. S., Hwang, K. T. and Kim, Ch. S., High-temperature strength and microstructural analysis in Si_3N_4/20 vol%–SiC nanocomposites. *J. Am. Ceram. Soc.*, 1999, **82**, 981–986.
8. Šajgalík, P., Hnatko, M., Lofaj, F., Hvizdoš, P., Dusza, J. and Warbicher, P., SiC/Si_3N_4 nano/micro-composite—processing, RT and HT mechanical properties. *J. Eur. Ceram. Soc.*, 2000, **20**, 453–462.
9. Munz, D. and Fett, T., *Ceramics: Mechanical Properties, Failure Behavior, and Materials Selection*. Springer Verlag, New York, 1996, p. 20.
10. Quinn, G. D. and Morrell, R., Design data for engineering ceramics: a review of the flexure test. *J. Am. Ceram. Soc.*, 1991, **74**, 2037–2066.
11. Weibull, W., *A Statistical Theory of the Strength of Mater*. Generalstabens Litografiska Anstalts Förlag, Stockholm, 1939.
12. Hertz, H.H., On the contact of elastic solids. *J. Reine. Angew. Math.*, 1881, 92, 156–171. Translated and reprinted in English, In *Hertz's Miscellaneous Papers*, ed. P. Lenard. Chs. 5 and 6. Authorized English translation by D. E. Jones and G. A. Schott. Macmillan, London, U.K., 1896.
13. Lawn, B. R., Indentation of ceramics with spheres: a century after Hertz. *J. Am. Ceram. Soc.*, 1998, **81**, 1977–1994.
14. Lawn, B. R., *Fracture of Brittle Solids* (*second ed.*). Cambridge University Press, Cambridge, 1993.
15. Warren, R., Measurement of the fracture properties of brittle solids by Hertzian indentation. *Acta Metall. Mater.*, 1978, **26**, 1759–1769.
16. Zeng, K., Breder, K. and Rowcliffe, D. J., The Hertzian stress field and formation of cone cracks. I. Theoretical approach. *Acta Metall. Mater.*, 1992, **40**, 2595–2600.
17. Zeng, K., Breder, K. and Rowcliffe, D. J., The Hertzian stress field and formation of cone cracks. II. Determination of fracture toughness. *Acta Metall. Mater.*, 1992, **40**, 2601–2605.
18. Warren, P. D., Statical determination of surface flaw distributions in brittle materials. *J. Eur. Ceram. Soc.*, 1995, **15**, 385–394.
19. Franco Jr., A. and Roberts, S. G., Surface mechanical analyses by Hertzian indentation. *Ceramics*, 2004, **50**, 94–108.
20. Kocer, C. and Collins, R. E., Angle of Hertzian cone cracks. *J. Am. Ceram. Soc.*, 1998, **81**, 1736–1742.
21. Fett, T., Munz, D. and Thun, G., Test devices for strength measurements of bars under contact loading. *J. Test. Eval.*, 2001, 29.
22. Fett, T., Munz, D. and Thun, G., *Strength and Toughness Test Devices with Opposite Roller Loading, Report FZKA 6378*. Forschungszen-trum, Karlsruhe, 2000.
23. Fett, T., Ernst, E. and Munz, D., Contact strength measurements of bars under opposite sphere loading. *J. Mater. Sci. Lett.*, 2002, **21**, 1955–1957.
24. Fett, T., Keller, R., Munz, D., Ernst, E. and Thun, G., Fatigue of alumina under contact loading. *Eng. Fract. Mech.*, 2003, **79**, 1143–1152.
25. Fett, T., Ernst, E., Rizzi, G., Munz, D., Badenheim, D. and Oberacker, R., Sphere contact fatigue of coarse grained Al_2O_3 ceramic. *Fatigue Fract. Eng. Mater.*, 2006, **29**, 876–886.
26. Fett, T. and Munz, D., Influence of stress gradients on failure in contact strength tests with cylinder loading. *Eng. Fract. Mech.*, 2002, **69**, 1353–1361.
27. Fett, T., Ernst, E., Munz, D., Badenheim, D. and Oberacker, R., Weibull analysis of ceramics under high stress gradients. *J. Eur. Ceram. Soc.*, 2003, **23**, 2031–2037.
28. Dusza, J. and Steen, M., Fractography and fracture mechanics property assessment of advanced structural ceramics. *Int. Mater. Rev.*, 1999, **44**, 165–216.
29. Danzer, R., Mechanical failure of advanced ceramics: the value of fractography. *Key Eng. Mater.*, 2002, **223**, 1–18.

30. Dusza, J. and Šajgalík, P., In *Fracture Characteristics of Layered and Nanoparticle Reinforced Si_3N_4. In Advanced Multilayered and Fibre Reinforced Composites*, ed. Y. M. Haddad. Kluwer Academic Publishers, 1998, pp. 187–205.
31. Kašiarová, M. and Dusza, J., Fractographic montage for a Si_3N_4–SiC nanocomposite. *J. Am. Ceram. Soc.*, 2006, **89**, 1752–1755.
32. Quinn, G. D., *Strength and Proof Testing. In Engineered Materials Handbook. Ceramics and Glasses*, *vol. 4*, ed. S. J. Schneider Jr. ASM International, Cleveland, 1991.
33. Hegedűsová, L., Contact strength and fatigue of ceramic materials. Ph.D. Thesis, Institute of Materials Research, Slovak Academy of Sciences, Košice, 2008.